Journal Homepage: http://ijcpe.uobaghdad.edu.iq
Iraqi Journal of Chemical and Petroleum Engineering
Vol. 27 No. 2 (June 2026) 33 – 43
EISSN: 2618-0707, PISSN: 1997-4884

Superior properties of drilling mud via sustainable nanoparticle priming

Hasan Ali Abbood [a, b, *], Zain-Ul-Abedin Arain [c], Sarmad Al-Anssari [a, b]

a Department of Chemical Engineering, College of Engineering, University of Baghdad, Iraq
b Department of Petroleum Engineering, College of Engineering, Al-Naji University, Iraq
c Western Australia School of Mines, Minerals, Energy and Chemical Engineering, Curtin University, 26 Dick Perry Avenue, Kensington 6151, WA, Australia

Abstract

This study demonstrates a sustainable, "trash-to-treasure" approach by synthesizing silica (SiO_2) and alumina (Al_2O_3) nanoparticles (30–80 nm) from local waste materials—specifically bentonite clay and aluminum wire waste—and evaluating their performance as eco-friendly additives in 350 mL water-based drilling fluids at concentrations ranging from 0 to 1 g. Tested under harsh subsurface conditions, the incorporated nanoparticles significantly enhanced the fluids' rheological properties, lubricity, filtration control, and swelling inhibition, with performance scaling alongside nanoparticle concentration. Notably, at a 1 g dosage, the fluid's yield point spiked from a baseline of 9 to 42 for SiO_2 and 32 for (Al_2O_3), while high-pressure high-temperature (HPHT) fluid loss was reduced from 21 mL to 14.6 mL (SiO_2) and 16.4 mL (Al_2O_3) due to the formation of a low-permeability filter cake. Furthermore, a 0.75 g dosage lowered the coefficient of friction from 0.45 to 0.35 (SiO_2) and 0.37 (Al_2O_3), while effectively mitigating clay swelling (SiO_2) showing superior inhibition at lower concentrations), ultimately proving that these waste-derived nanoparticles offer a highly effective, cost-efficient, and environmentally friendly alternative to commercial drilling mud additives.

Keywords: Sustainable synthesis; silica; alumina; nanoparticles; drilling mud.

Received on 17/03/2026, Received in Revised Form on 01/06/2026, Accepted on 01/06/2026, Published on 30/06/2026

https://doi.org/10.31699/IJCPE.2026.2.3

1- Introduction

Global energy demand has continuously increased over the past few decades. This scenario has prompted the oil and gas industry to focus on developing more complex and challenging reservoirs, such as unconventional shales. Unique characteristics of these reservoirs include their exceedingly low permeability and nanometer-sized pore throats [1]. Shale reservoirs are considered the main source of fossil fuels due to the depletion of conventional hydrocarbon reservoirs.

Over the past ten years, the United States has seen an increase in the extraction of gas and oil from shale deposits. The shale reservoirs are mostly made of porous sedimentary rock and are extremely vulnerable to hydration and swelling as a result of contact with drilling mixtures [2]. Drilling fluid's primary functions include maintaining stable borehole conditions, lubricating and cooling drill bits, reducing damage to the productive zone, preventing cuttings from sticking to downhole equipment, and removing drill cutting [3, 4].

Nanotechnology has a wide range of potential uses in the oil and gas sector, some of which could pave the way for the discovery of hitherto untapped hydrocarbon reservoirs in sedimentary basins. This method can improve the drilling fluid's macroscopic features, including its rheological, filtration, mechanical, and thermal behavior, for optimal drilling performances [5, 6]. Their potential usefulness in improving viscosity and reducing fluid loss in drilling fluid rheology stems from their strong interparticle interaction [7].

The specific gravity of the fluid in which the nanoparticles were mixed was increased by using densification agents, which are nanoparticles. It is possible for the completion fluid to eliminate the skin caused by the mud cake, resulting in enhanced effectiveness. Nanoparticles can be used to plug fractures in a wellbore, which can add integrity to the wellbore and reduce the amount of mud that is lost throughout the course of drilling [8]

One of the most common nanomaterials used in WBMs is silica nanoparticles because of its many useful properties, including a large surface area, controlled size, dispersibility, and surface features that aid in reducing water invasion during formation and modifying rheology and filtration characteristics [9]. In addition, multiple investigations have demonstrated that water-based muds enriched with silica nanoparticles (ranging from 0.1% to 0.3% by weight) have enhanced characteristics. Furthermore, by demonstrating its ability to resolve drilling and production issues, they demonstrated its viability as an alternative to oil-based mud in directional,

*Corresponding Author: Email: hasan.abbood1607m@coeng.uobaghdad.edu.iq

horizontal, and rocky drilling operations. Further, they found that it had the potential to improve the characteristics of high-pH drilling mud [10]. The erosion and cracking along the boundary and in the center of the shale plug are less severe when submerged in Al_2O_3 NPs mud as compared to basic mud. On the other hand, the Al_2O_3 NPs mud system exhibits better shale inhibition than the Fe_2O_3 NPs mud system [11, 12]

Therefore, aims to investigate the optimal concentrations of silica SiO_2 and alumina Al_2O_3 NPs, both singly and synergistically, in the drilling mud to achieve the best lubricity, rheological behavior, and swelling using a permeable plugging tester, a high-temperature high-pressure fluid loss apparatus, and an API low-temperature low-pressure fluid loss device. Furthermore, the NPs (e.g., SiO_2 and Al_2O_3 NPs) used in this study were synthesized from sustainable sources and directly utilized in the experiment to minimize the potential impact of contamination on the acquired results. To the best of our knowledge, this is the first insight into the effect of NPs on drilling mud properties at subsurface conditions. Some other gradients listed in Fig. 1, were typically used to prevent water absorption and loss of drilling fluid.

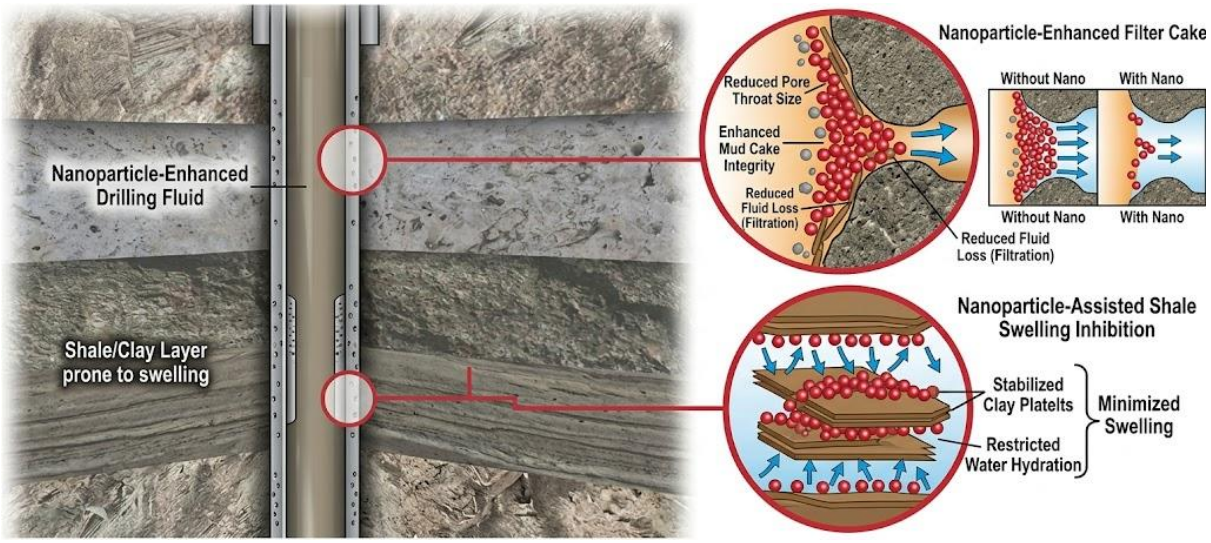

Fig. 1. Nanoparticles seal wellbore fractures, minimizing drilling mud loses.

2- Materials and methods

2.1. Materials

Waste bentonite was delivered by PetroChina Halfaya FZCO, Iraq Branch, the field's official operator, pursuant to licensing rounds concluded by the Iraqi Ministry of Oil with foreign companies. Such waste bentonite from drilling activities requires costly storage space, adding an additional cost to the project. This bentonite can be considered a sustainable source for producing silica nanoparticles, as a kind of trash-to-treasure strategy. DI water (conductivity = 1 μS/cm) was purchased from the local market and used in various processes in this study, including preparing the mud, synthesizing nanoparticles, various neutralization and cleaning protocols. Xanthan gum drilling mud, also known as a polysaccharide $((C_{35}H_{49}O_{29})_n)$, was gifted by CNOOC (China National Offshore Oil Corporation), Iraq Limited. Xanthan gum is a hydrocolloid polymer used with water and other additives, including starch, PAC-LV (Polyanionic Cellulose, and KOH, to formulate viscous and stable drilling mud. Furthermore, acidity-control reagents, hydrochloric acid (HCl, 33%) and sodium hydroxide (NaOH, Mol.wt =39.997 g/mol), were purchased from the local Iraqi market and used without further purification. Ethanol (C_2H_5OH, purity ≥ 99.0%, boiling point 78.37°C, from Sasma premium) was the cosolvent of the NPs preparation methods.

2.2. Sustainable preparation of silica NPs

Iraqi oil fields produce considerable amounts of bentonite waste resulting from well-drilling activities. This waste contains a high proportion of phyllosilicates, which are rich in silicon, providing a significantly low-cost source of silica NPs. Such abundant, low-cost, byproduct bentonite assures the sustainability of SiO_2 NPs production. To achieve this, the bentonite was first filtered through a 100 μm mesh to guarantee a narrow particle size distribution of the raw material. It was then dried in a muffle furnace at 680°C for one hour. Subsequently, to achieve a silica-rich sample, 100 g of clay was mixed with 1000 mL of 2.5 M HCl solution and stirred at 90°C for 2 hours. After multiple filtering steps, the mixture was subjected to sufficient washing with DI water until it reached a neutral pH. Here, two silica-silicate aqueous phases were formulated by mixing bentonite at various contents (e.g., 10% and 40%) with 2 mol/L sodium hydroxide solution for 120 minutes at 90°C in separate processes. Each mixture was then filtered to remove residues and impurities, followed by neutralization with nitric acid in the presence of excess ethanol at 50°C. The solution was subsequently

centrifuged using a Lab Benchtop Centrifuge (Electric 96-Well Plate Spinner, 500-2000 RPM Low-Speed Centrifuge) at 1800 rpm for half an hour to disperse the solid silica from the mixture. After discarding the liquid phase, the remaining silica was heated to 105°C for 3 hours to achieve dry silica NPs [13].

2.3. Sustainable synthesis of Al_2O_3 NPs from aluminum waste

The second implementation of the trust-to-treasure strategy is the sustainable preparation of alumina NPs from aluminum scrap. In this context, valuable alumina NPs were produced from aluminum waste, thereby reducing the critical environmental impact of these wastes through recycling this expensive metal. For this purpose, aluminum fillings were initially cut into small pieces and duplicated at a very small size. Such a small size increases the surface area, facilitating the chemical reaction and helping to control the required size of the reaction vessel. The fillings were subsequently aged in acetone for degreasing, further cleaned in an ultrasonic cleaner with a liquid detergent for half an hour, and flushed with water. This process cleaning protocol was repeated twice to ensure efficient cleaning and high-purity products. To prevent overheating, 4.5 g of cleaned fillings were added very slowly to 250 mL of 2 M hydrochloric acid in a corrosive-resistant vessel under efficient venting. The intermediate product from Eq.1, aluminum chloride ($AlCl_3$), during dissolution was then filtered to eliminate all undissolved fillings from the liquid phase. Next, an adequate amount of 5 M NaOH solution was added dropwise to the liquid phase to formulate a gel of Al $(OH)_3$, as indicated in Eq. 2. This gel was separated from the brine and rinsed with DI water at 80°C to facilitate detachment of the generated NaCl. Eventually, $Al(OH)_3$ was heated to 1000°C for 60 minutes to remove the remaining water, yielding Al_2O_3 powder (Eq. 3). To obtain nano-sized alumina, the produced powder was milled at 550 rpm for two days [14].

$$2Al + 6HCl \rightarrow 2AlCl_3 + 3H_2 \quad (1)$$

$$2AlCl_3 + 3NaOH \rightarrow Al(OH)_3 + 3NaCl \quad (2)$$

$$2Al(OH)_3 \xrightarrow{\frac{Heat}{1000°C}} Al_2O_3 + 3H_2O \quad (3)$$

2.4. Drilling formulations

A base drilling formulation (BF) consisting of 5% bentonite in deionized (DI) water was prepared using a mechanical mixer. Experimentally, the mechanical mixing is continued for 24 hours to achieve homogeneous clay dispersion. Characteristically, two categories of enhanced drilling mud were then formulated: BN and BP. The BN was prepared by directly adding solid silica and alumina NPs, separately, to the BF at various loads ranging between 0.25g and 1 g. The other category (BP) was prepared by adding silica or alumina nanofluids separately to the BF at various nanofluid concentrations. The goal of such formulations was to examine the combined influence of NPs on filtration characteristics, rheological behavior, and shale inhibition [15].

2.5. Characterization

2.5.1. XRD and FTIR nanoparticles

The crystalline structure of NPs was ascertained by analyzing the XRD pattern with the Rigaku Ultima IV equipment. To examine the functional groups and chemical bands found in the materials, the PerkinElmer Spectrum 100 device was used in transmission mode to perform FT-IR spectroscopy analysis of silica and alpha alumina NPs. This analysis covered the wavenumber range of 400 - 4000 cm^{-1} with a resolution of 2 cm^{-1}[16].

2.5.2. Morphological test

The FESEM-TESCAN-XMU model of scanning electron microscopy was used to evaluate the structure and elemental makeup of the produced NPs in this investigation [17].

2.5.3. Atomic force microscope

Atomic Force Microscope (AFM-LN Digital Instruments, ARTISAN technology group) measurements were utilized to confirm the nano-nature of the synthesized particles, with their topography [18].

2.5.4. Rheological testing

The flow characteristics of the mixed muds were systematically studied. Properties, including thickness, strength of cohesion, thickness of the solid material layer, and the amount of liquid lost, were systematically measured under various operational conditions. A Van-G meter was employed to evaluate gel strength (10 minutes) and mud viscosity (10 seconds). The yield point (YP) (Eq. 4), gel strength (GS), and plastic viscosity (PV) criteria were all established in accordance with the API standard (Eq. 5). The PV and yield point values at motor speeds of 300 RPM and 600 RPM were assessed using the Van-G meter. The filter cake was subsequently evaluated, and a filter press was employed to ascertain the filtration loss. A pressurized filter medium is located within the pressurized cells of the filter press. To raise the cell pressure to 100 psi, a nitrogen cylinder was connected to the filter press device. An Ofite HTHP filter press was utilized to conduct the high-pressure high-temperature filtration test at 120°C and 500 psi. This technique utilized standard filter paper and CO_2 to generate pressure. Each of the two tests required approximately 30 min [19].

$$PV = \theta_{600} - \theta_{300} \quad (4)$$

$$YP = \theta_{300} - PV \quad (5)$$

2.5.5. Lubricity

The coefficient of friction (COF) was measured during the lubricity test using extreme pressure/lubricity testers. The drill string and wellbore are similar in that they are both made of metal [20]. An estimation of lubricity might be conducted via the (Eq. 6) below:

$$CoF = \frac{Torque\ reading}{100} \quad (6)$$

2.5.6. Testing shale swelling

To prevent shale formation swelling, drilling muds should be intended to deliver the best possible reserve and well stability. A clay-rich formation may expand rapidly during drilling if the drilling mud is not appropriate for that formation. Shale instability, washouts, clogged pipes, and constricted holes may result from this swelling. The well stability improves via an appropriate drilling mud prior or during drilling. We used a technique to measure expansion to track the length of a quality shale core over time at normal temperature and pressure to see if the shale was absorbing or losing water. The swelling was measured in millimeters and given as a percentage of the initial length. The percentage indicator shows how much the pressed shale powder in the fluid cup has expanded, applying pressure to the pipe [21].

3- Results and discussion

3.1. Characterization of nanoparticles

3.1.1. The XRD patterns

Fig. 2 (A) illustrates the XRD pattern of the synthesized silica nanoparticles. XRD results detected a broad peak instance at 2θ = 23°, with some variation (20-25°) depending on the synthesis conditions and water content. Other short-range order attributes to the Si-O-Si bond angles and distance. With no other significant peaks. These results confirm the amorphous nature of silica NPs The XRD pattern of Al_2O_3 NPs are depicted in Fig. 2 (B). Diffraction bands were observed at 2θ values of 27°, 33°, 37.7°, 46°, 56.4°, 65°, 75.5°, and 84.9°, respectively. All of the detected diffraction peaks coincide with specific Miller indices: 120, 108, 118, 012, 290, 024, 130, and 224. With the card $number\ 00-010-0173$, these indices are an exact match to the reference pattern for Al_2O_3 in the ICDD database. According to the diffraction examination, the produced nanoparticles have a hexagonal lattice structure [16].

3.1.3. FE-SEM analysis

The FE-SEM pictures of silica nanoparticles, shown in Fig. 3A, have a constant, almost spherical shape. For silica nanoparticles, the most common distribution of particle sizes is around 92 nm. Fig. 3B, shows pictures of alumina nanoparticles captured by FE-SEM. The morphologies of these alumina nanoparticles ranged from spherical to semi-spherical, and their crystal sizes varied. In addition, the photos indicate the existence of aggregates made up of many nanoparticles. For alumina nanoparticles, a 44 nm dispersion is the most typical. Because of their tiny size and enormous surface area, nanoparticles are able to successfully cross microscopic holes and mobilize contained oil. This leads to a dramatic improvement in oil recovery.

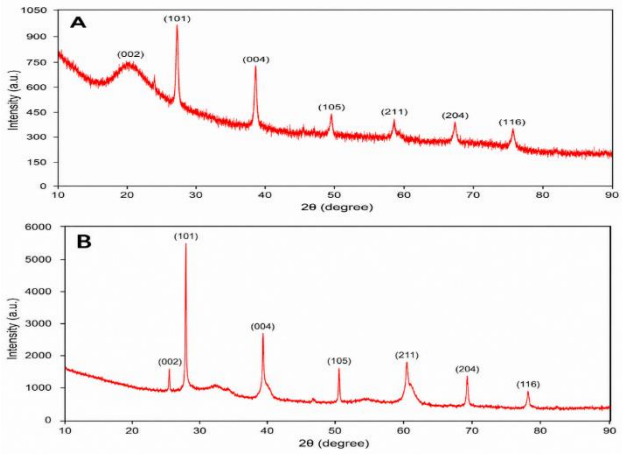

Fig. 2. shows the XRD patterns for silica nanoparticles(A) made at 600°C, which have a non-crystalline structure, and alumina nanoparticles(B) made at 1200°C

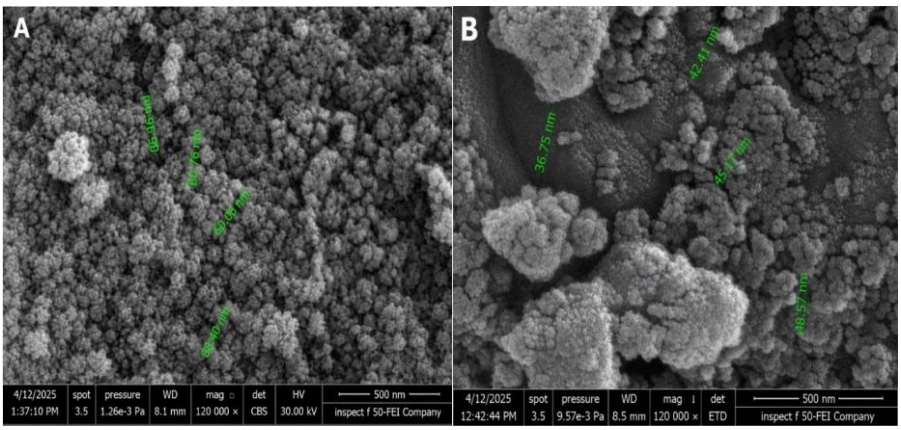

Fig. 3. FE-SEM images for silica NP (A), and alumina NPs (B)

3.1.2. FT-IR analyses

This examination focuses on the relationship between the sample's chemical composition and its absorption bands, particularly its vibrational bands [22]. Fig. 4A, displays the FTIR transmittance spectrum, providing evidence of the existence of the synthesized silica nanoparticles, spanning 400-4000 cm^{-1}. O-H stretching vibrations are reflected in a band from 1637 to 1620 cm^{-1}, while O-H groups are responsible for the broad feature between 3415 and 3443 cm^{-1}. In addition, the results from Adam and Chua are in agreement that high temperatures are necessary for the total elimination of water molecules. In addition, the significant bands at 1103 and 802 cm^{-1} represent the stretching vibrations of Si-O-Si, whereas the feature at 459 cm^{-3} signifies the Si-O bond. The FTIR spectra of the alumina nanoparticles that were synthesized is shown in Fig. 4B. Aluminum and oxygen atomic vibrations are corresponding to the bands at 440 and 894 cm^{-1}. Even more so, the band in the 3450-3650 cm^{-1} range is produced by the bending and stretching vibrational modes of a water molecule [23].

3.1.4. AFM analyses

Fig. 5, provided additional information about the surface and size of the materials. The silica nanoparticles Fig. 5A, showed a well-organized surface, with an average particle size of 7.35 nm for samples made with 5 M HNO_3. This size is consistent with what has been reported in Tadanaga et al [24]. In contrast, the alumina nanoparticles Fig. 5B, had a smooth and even surface, with an average size of 2.79 nm. FM analysis further revealed that approximately 30% of the alumina nanoparticles exhibited a particle size of 58 nm, while the remaining 70% displayed a diameter of 16 nm. This observed uniformity indicates a significant potential for application as efficient adsorbents and catalytic agents, thereby supporting conclusions drawn from prior research Mirzaasadi et al [25]. In summary, the multimodal characterization validates the successful synthesis of nanoscale silica and alumina particles, each possessing unique structural, chemical, and morphological characteristics, which are appropriate for the functional improvement of water-based drilling fluids [26].

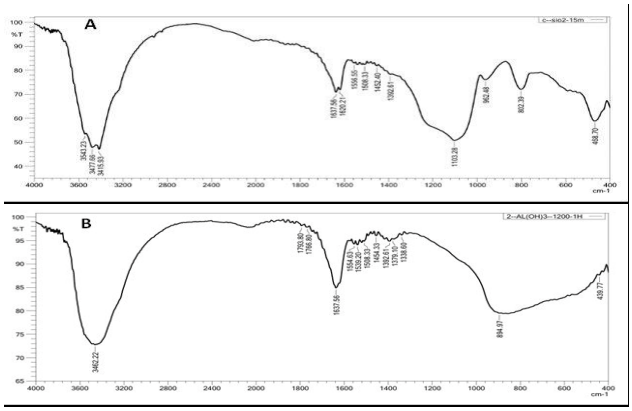

Fig. 4. FTIR spectra patterns for silica NPs (A) and alumina NPs (B)

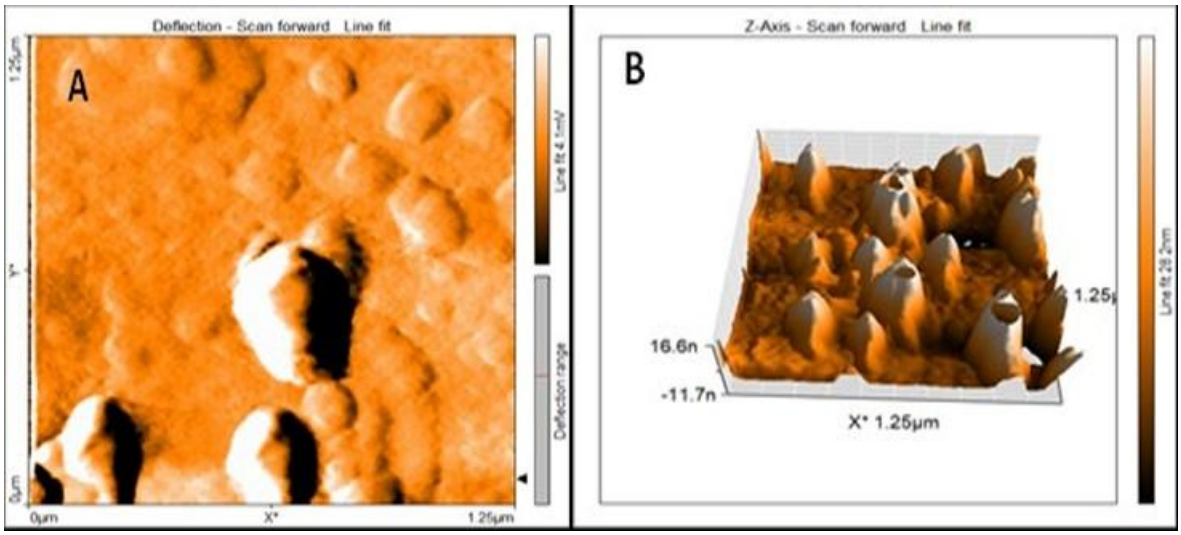

Fig. 5. FE-SEM images for silica NPs (A) and alumina NPs (B)

3.2. Properties of rheology

3.2.1. Plastic viscosity

Plastic viscosity (PV) is a fluid's resistance to flow. It's mainly due to the interaction of adjusted particles in the drilling mud, which causes mechanical friction, the liquids, and the deformation of the liquid that is under shear stress [27]. For this reason, drillers rarely use drilling fluids with a high PV in actual drilling operations. The addition of NPs generally increased the PV of Bentonite-WBM, as shown in Fig. 6, which shows that the base fluid displayed a plastic viscosity of 7 cP. The viscosity remained constant at 7cP with (0.25 and 0.5g) of SiO_2 NPs but increased to a maximum of 8cP at (0.75 and1g). Additionally, Al_2O_3 NPs increased PV more than

SiO_2 NPs when added to the base fluid. The viscosity gradually increased to 9 *cP* at 0.5 and 0.75g, respectively, but become 10cP at 1 g, coordinating with Maulani et al [28]. The results obtained from Al_2O_3 NPs were notably different from those of SiO_2 NPs. The plastic viscosity of the nano-based formulations was discovered to be slightly higher for Al_2O_3 NPs based mud formulations and to remain between 7 and 8 cP for SiO_2 NPs based formulations, which agrees with available literature Abbood & Al-Anssari [29, 30].

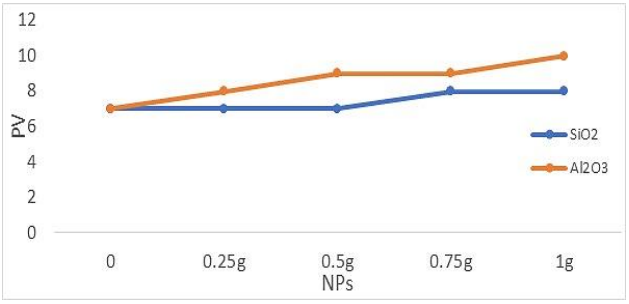

Fig. 6. NPs concentration affected by Plastic Viscosity (cp)

3.2.2. Yield point

In the Bingham plastic model, Yield Point (YP), the initial resistance to flow induced by electrochemical forces between particles, is a crucial parameter influenced by the volume fraction of solids and the surface properties of the particles. A mud's capacity to lift cuttings out of the annulus under dynamic conditions is assessed using its yield point [31]. During testing, the xanthan-WBM's YP was measured at 4 lb/100ft^2. Fig. 7, illustrates how NPs can affect the (YP) of xanthan-WBMs. Firstly, the yield point of base mud was measured at 15 lb./100 ft², subsequently growing to a peak of 48 lb./100 ft^2 after incorporating 1 g of Al_2O_3 NPs that are listed in Ahmed Hullio et al [32]. The yield point for SiO_2NPs was observed at 26 lb./100 ft² with a load of 0.3 g, rising to a highest of 58 lb./100 ft² at 1 g.

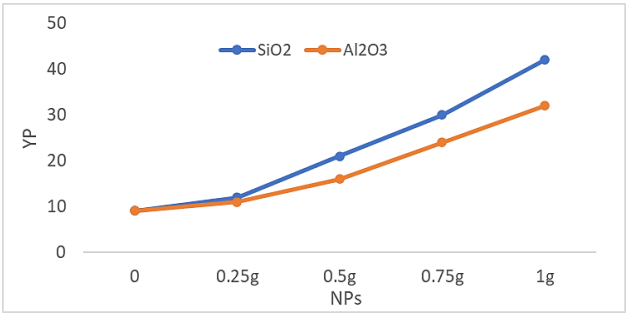

Fig. 7. NPs concentration affects the yield point

3.2.3. Gel strength

A crucial mud feature is gel strength, which shows how well the drilling fluid can suspend drill cuttings and weighing elements after circulation is stopped [33]. The impact of NPs on gel strength is illustrated in Fig. 8 and Fig. 9 at 10 seconds and 10 minutes, respectively. The gel strength of base mud was measured at 10 seconds and 10 minutes, yielding values of 3.5 lb/100 ft² and 8 lb/100 ft², respectively. The gel strength of Bentonite-WBM increased with the addition of Al_2O_3 NPs, ranging from 0.25 to 1 g, as listed in Deng et al [34]. The gel strength of Bentonite-WBM at 10 seconds and 10 minutes was measured at 28 and 32 lb/100 ft², respectively, with a concentration of 1 g Al_2O_3 NPs. Following 10 seconds and 10 minutes of exposure to SiO_2 NPs, the gel strengths elevated to 34 and 38 lb/100 ft², respectively, which indicated Doukeh et al [35]. A greater initial torque may be necessary to accommodate the fluid's pronounced gelling properties. A robust gel is necessary to prevent numerous challenging drilling scenarios finally, at 1 g concentration, SiO_2NPs gel better than Al_2O_3 NPs.

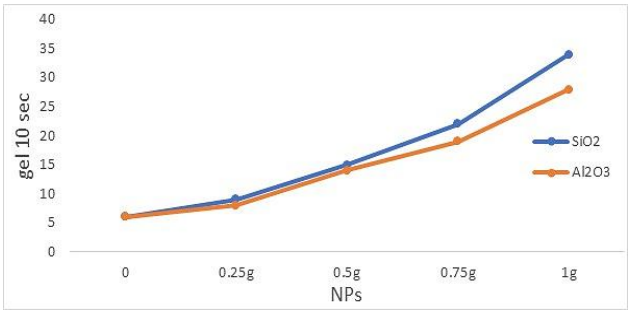

Fig. 8. NPs concentration effects on gel strength over a 10-sec

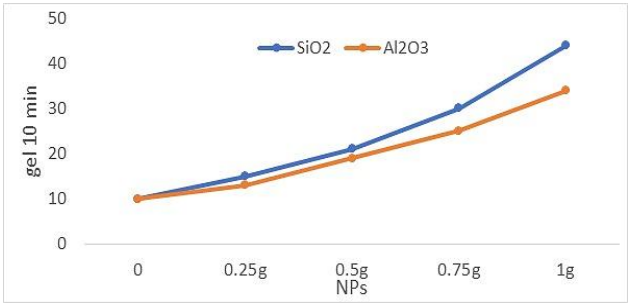

Fig. 9. NPs concentration effects on gel strength over a 10-minute period.

3.3. Influence of nanoparticles on fluid filtration

In this test, it is possible to determine how much fluid has been lost and how thick the mud cake has become. High filter loss is undesirable because it can cause damage and instability during the forming process [36]. Fig. 10 and Fig. 11 demonstrate the filtration efficiency of the Bentonite-WBM under (a) ambient conditions (LTLP) and (b) subsurface harsh (HTHP) conditions. The outcomes show that the base mud displayed filtrate volumes of 12.4 mL at LTLP and 21mL at HPHT. The addition of 0.25 g of silica NPs reduced the filtrate volumes to 10.2 ml at LTLP and 13.6 ml at HPHT. In contrast, the combination of base mud and silica NPs showed improved performance more than alumina NPs. A gradual decrease was observed at 0.5 g, ultimately resulting in filtrate volumes of 8ml and 9.8 ml at 1 g. In

both LTLP and HTHP conditions reported in Wang et al [37]. Adding 0.25 g of alumina NPs reduced the filtrate volumes by 10.4 ml and 14.6 ml, while using 0.5 g of alumina NPs with the base mud directed to greater decreases to 9.2 ml and 11.2 ml. The influences of LTLP and HTHP are examined in relation to the base fluid. SiO_2 NPs performed better than Al_2O_3 NPs, but both kinds facilitated the reduction of the liquid that passed through. The hydration of mud minerals by Al_2O_3 and SiO_2 NPs occurs because these NPs limit the quantity of water that may enter the gaps among clay particles, thereby effectively preventing shale issues [38].

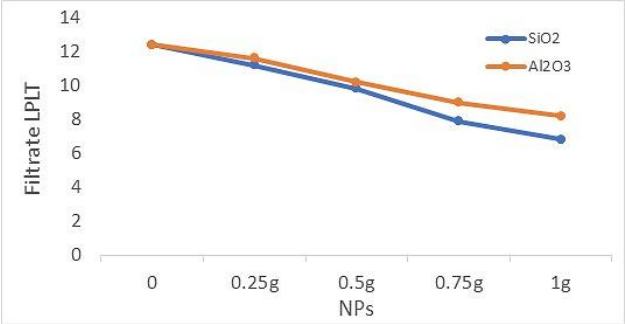

Fig. 10. NPs concentration affects the filtrate (ml)

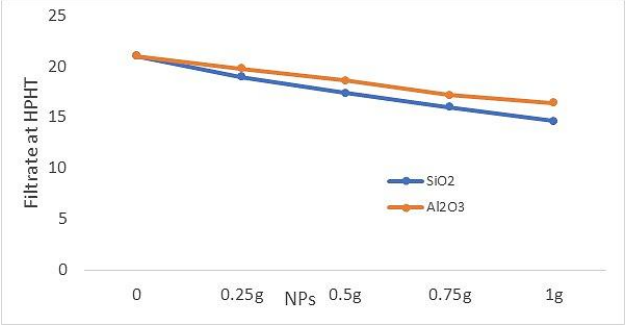

Fig. 11. NPs concentration affects the filtrate (ml)

3.4. Swelling behavior and nanoparticle effects

By decreasing syneresis and improving their swelling behavior, higher concentrations of silica and alumina NPs enhanced the bentonite WBM during the swelling evaluation of the base mud and NPs. Consequently, the best silica-based WBM was identified as silica NPs. On the other hand, an increase in alumina NPs concentration during the swelling evaluation of the bentonite WBM and alumina NPs resulted in syneresis in addition to reducing the swelling of the polymer gel. Fig. 12, using four different drilling fluids, shows the expansion meter results for sodium bentonite shale, including fresh water, Al_2O_3 and SiO_2 NPs, Xanthan-WBM. After 18 hours of exposure to fresh water, the xanthan-WBM grew by 7.32%, as agrees with Miao et al [39] .The addition of SiO_2 nanoparticles reduced shale swelling in water-based drilling fluid to below 4%. The incorporation of Al_2O_3 nanoparticles reduces swelling to 4.90% by effectively occluding nanopores in clay, hence inhibiting shale expansion. Due to stability concerns, Bentonite-WBM fails to sufficiently diminish swelling; however, this can be alleviated by incorporating Bentonite-WBM with the nanoparticles. The synergetic effects of nanoparticles indicate that the bentonite in the nanoparticle system absorbed less water, leading to less clay swelling and enhanced shale strength [40].

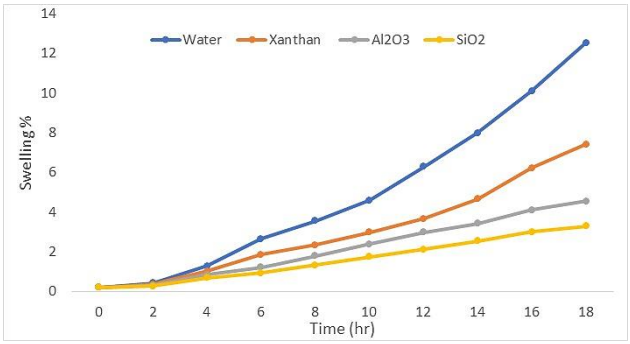

Fig. 12. Exposed to fresh water and drilling fluids, sodium bentonite's swelling percentage

3.5. Lubricity and nanoparticle concentration

Drag and torque are both affected by the coefficient of friction (CoF). Precise correlations between field and lab data are essential for CoF. Low CoF is necessary for the design of well paths and drill strings, as well as for the creation of mud systems that can reduce drag and torque. This shows that the fluid is lubricating well Komekbay et al [41] .This study found that a small amount of nanoparticles in the drilling fluid slightly decreased CoF, Fig. 13. SiO_2 NPs typically have a greater surface area than Al_2O_3 NPs. SiO_2 and Al_2O_3 NPs were added to xanthan-WBM at 0.75g each, reducing torque to 35% and 37%, respectively. However, 1g of Al_2O_3 NPs produced the highest torque of 40%. Because it crushes more readily when rotating, xanthan-WBM has higher CoF values than Bentonite-WBM with SiO_2 NPs and Al_2O_3 NPs, as presented in Fan et al [42].

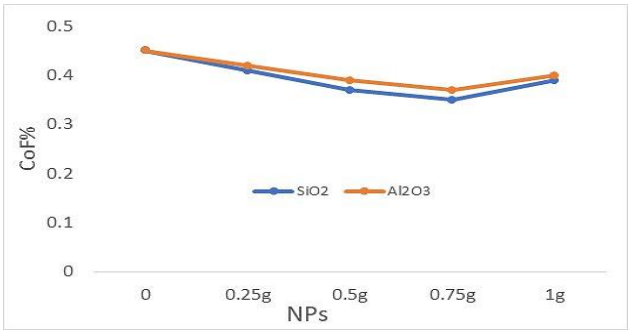

Fig. 13. NPs concentration effects on the coefficient of friction (CoF)

4- Conclusion

Feasible enhancement of drilling mud properties can be achieved via adding sustainably synthesized nanoparticles from zero-cost raw materials. Characterization analyses (XRD, FTIR, AFM, FESEM) confirmed the successful synthesis of SiO_2 and Al_2O_3 nanoparticles with particle

sizes of 30–80 nm and acceptable purity, and verified the crystalline structure and distinctive functional groups for each type. The incorporation of nanoparticles significantly improved the rheological properties of the drilling fluids. Increases in plastic viscosity, yield point, and gel strength were observed with increasing nanoparticle concentration, attributed to the high surface area of nanoparticles and the development of a structured network within the fluid that enhances cohesion and stability. A marked reduction in the coefficient of friction was achieved, particularly at 0.75 g addition, where the lowest values were recorded (0.35 for SiO_2 and 0.37 for Al_2O_3). This reduction can lower torque and drag during drilling operations, thereby improving drilling efficiency. Filtration properties were substantially enhanced under both LPLT and HPHT conditions. The HPHT filtrate volume decreased from 21 mL (reference) to 14.6 mL for SiO_2 and 16.4 mL for Al_2O_3 at 1 g concentration. This improvement is attributed to the nanoparticles' ability to plug pores and form a thin, low-permeability filter cake that minimizes fluid invasion into formations. The nanoparticles effectively reduced the swelling percentage compared to water alone.

References

[1] J. Aramendiz and A. Imqam, "Water-based drilling fluid formulation using silica and graphene nanoparticles for unconventional shale applications," *Journal of Petroleum Science and Engineering*, vol. 179, pp. 742–749, 2019. https://doi.org/10.1016/j.petrol.2019.04.085

[2] H. M. Ahmad, T. Iqbal, M. A. Al Harthi, and M. S. Kamal, "Synergistic effect of polymer and nanoparticles on shale hydration and swelling performance of drilling fluids," *Journal of Petroleum Science and Engineering*, vol. 205, Oct. 2021. https://doi.org/10.1016/j.petrol.2021.108763

[3] J. A. Ali et al., "Evaluation the effect of wheat nano-biopolymers on the rheological and filtration properties of the drilling fluid: Towards sustainable drilling process," *Colloids and Surfaces A: Physicochemical and Engineering Aspects*, vol. 683, Feb. 2024. https://doi.org/10.1016/j.colsurfa.2023.133001

[4] H. A. Abbood and I. K. Shakir, "Using nano-additives to improve drilling fluid properties," *AIP Conference Proceedings*, vol. 2779, 2023. https://doi.org/10.1063/5.0142334

[5] S. Perween, M. Beg, R. Shankar, S. Sharma, and A. Ranjan, "Effect of zinc titanate nanoparticles on rheological and filtration properties of water based drilling fluids," *Journal of Petroleum Science and Engineering*, vol. 170, pp. 844–857, 2018. https://doi.org/10.1016/j.petrol.2018.07.006

[6] V. A. Zhigarev, M. I. Pryazhnikov, A. V. Matveev, E. I. Mikhienkova, and D. V. Guzei, "Computational study of cutting transport by drilling fluids in directional wells," *Journal of Physics: Conference Series, IOP Publishing Ltd*, Dec. 2020. https://doi.org/10.1088/1742-6596/1677/1/012079

[7] G. N. Abang, Y. S. Pin, and N. Ridzuan, "Application of silica (SiO_2) nanofluid and Gemini surfactants to improve the viscous behavior and surface tension of water-based drilling fluids," *Egyptian Journal of Petroleum*, vol. 30, no. 4, pp. 37–42, Dec. 2021. https://doi.org/10.1016/j.ejpe.2021.10.002

[8] A. Retnanto et al., "Evaluation of the viability of nanoparticles in drilling fluids as additive for fluid loss and wellbore stability," *Petroleum*, vol. 9, no. 3, pp. 342–351, Sep. 2023. https://doi.org/10.1016/j.petlm.2023.02.005

[9] Y. Villada et al., "Synergistic effect of nanoparticles and viscoelastic surfactants to improve properties of drilling fluids," *Petroleum Science*, vol. 21, no. 6, pp. 4391–4404, Dec. 2024. https://doi.org/10.1016/j.petsci.2024.11.014

[10] A. K. Alkalbani, G. T. Chala, and A. M. Alkalbani, "Experimental investigation of the rheological properties of water base mud with silica nanoparticles for deep well application," *Ain Shams Engineering Journal*, vol. 14, no. 10, p. 102147, 2023. https://doi.org/10.1016/j.asej.2023.102147

[11] K. Al Attabi et al., "Enhanced Rheological and Filtration Performance of Drilling Fluids Using Fe_3O_4/Saponin/Cu(II) Nanocomposites: Synthesis, Characterization, and Application," *Asia-Pacific Journal of Chemical Engineering*, 2026. https://doi.org/10.1002/apj.70234

[12] M. S. Hameed, N. S. Al-Zubaidi, and A. A. Alwasiti, "Multi-Functional Enhancement of Water-Based Drilling Fluid Using Copper Nanoparticles: A Study on Lubricity, Rheology, and Filtration Properties," *Emerging Trends in Engineering and Sustainability*, vol. 2, no. 1, pp. 13–20, Mar. 2026. https://doi.org/10.65505/ETES-25-0013

[13] U. Zulfiqar, T. Subhani, and S. W. Husain, "Synthesis and characterization of silica nanoparticles from clay," *Journal of Asian Ceramic Societies*, vol. 4, no. 1, pp. 91–96, 2016. https://doi.org/10.1016/j.jascer.2015.12.001

[14] M. Esaifan et al., "Synthesis of Nanostructured Alumina from Byproduct Aluminum Filings: Production and Characterization," *Inorganics*, vol. 11, no. 9, 2023. https://doi.org/10.3390/inorganics11090355

[15] A. R. Albajalan and H. K. Haias, "Evaluation of the Performance of Conventional Water-Based Mud Characteristics by Applying Zinc Oxide and Silica Dioxide Nanoparticle Materials for a Selected Well in the Kurdistan/Iraq Oil Field," *Advances in Materials Science and Engineering*, vol. 2021, 2021. https://doi.org/10.1155/2021/4376366

[16] B. M. Kurji, I. M. Mujtaba, and A. S. Abbas, "Synthesis, Characterizations, and Recent Applications of the Silica-based Mobil Composition of Mesoporous Material: A Review," *Iraqi Journal of Chemical and Petroleum Engineering*, vol. 24, no. 3, pp. 1–12, 2023. https://doi.org/10.31699/ijcpe.2023.3.1

[17] N. A. Al-Rubaiey, F. S. K. Kadhim, and M. G. A. Albrazanjy, "The Effect of Adding Carboxymethyl Cellulose and Zinc Sulfate on the Corrosion Characteristics of the Drilling Fluid," *Al-Khwarizmi Engineering Journal*, vol. 15, no. 1, pp. 125–133, Mar. 2019. https://doi.org/10.22153/kej.2019.08.003

[18] X. Wang et al., "Research on Nanoparticle-Enhanced Cooling Technology for Oil-Based Drilling Fluids," *Applied Sciences*, vol. 14, no. 23, pp. 1–12, 2024. https://doi.org/10.3390/app142310969

[19] A. I. El-Diasty and A. M. Salem Ragab, "Applications of nanotechnology in the Oil & Gas industry: Latest trends worldwide & future challenges in Egypt," *SPE North Africa Technical Conference and Exhibition* (SPE-164716-MS), 2013. https://doi.org/10.2118/164716-ms

[20] J. O. Oseh, M. N. A. Mohd Norddin, I. Ismail, A. O. Gbadamosi, A. Agi, and H. N. Mohammed, "A novel approach to enhance rheological and filtration properties of water–based mud using polypropylene–silica nanocomposite," *Journal of Petroleum Science and Engineering*, vol. 181, p. 106264, 2019. https://doi.org/10.1016/j.petrol.2019.106264

[21] R. Rafati, S. R. Smith, A. Sharifi Haddad, R. Novara, and H. Hamidi, "Effect of nanoparticles on the modifications of drilling fluids properties: A review of recent advances," *Journal of Petroleum Science and Engineering*, 2018. https://doi.org/10.1016/j.petrol.2017.11.067

[22] S. Jarmolińska, A. Feliczak-Guzik, and I. Nowak, "Synthesis, characterization and use of mesoporous silicas of the following types SBA-1, SBA-2, HMM-1 and HMM-2," *Materials*, vol. 13, no. 19, pp. 1–33, 2020. https://doi.org/10.3390/ma13194385

[23] Q. A. Mahmood, B. A. Abdulmajeed, and R. Haldhar, "Oxidative Desulfurization of Simulated Diesel Fuel by Synthesized Tin Oxide Nano-Catalysts Support on Reduced Graphene Oxide," *Iraqi Journal of Chemical and Petroleum Engineering*, vol. 24, no. 4, pp. 83–90, 2023. https://doi.org/10.31699/ijcpe.2023.4.8

[24] K. Tadanaga, K. Morita, K. Mori, and M. Tatsumisago, "Synthesis of monodispersed silica nanoparticles with high concentration by the Stöber process," *Journal of Sol-Gel Science and Technology*, vol. 68, no. 2, pp. 341–345, 2013. https://doi.org/10.1007/s10971-013-3175-6

[25] M. Schneider, K. Cesca, D. Amorim, R. F. P. M. Moreira, D. Hotza, and E. Rodrigues, "Synthesis and characterization of silica-based nanofluids for enhanced oil recovery," *Journal of Materials Research and Technology*, 2023. https://doi.org/10.1016/j.jmrt.2023.04.049

[26] M. Mirzaasadi, V. Zarei, M. Elveny, S. M. Alizadeh, V. Alizadeh, and A. Khan, "Improving the rheological properties and thermal stability of water-based drilling fluid using biogenic silica nanoparticles," *Energy Reports*, vol. 7, pp. 6162–6171, 2021. https://doi.org/10.1016/j.egyr.2021.08.130

[27] Z. E. M. ALZubaidi, F. H. M. Almahdawi, and Y. M. F. Mukhtar, "Enhance the rheological properties of reservoir drilling fluid (RDF) using Fe_2O_3 as nanoparticle material," *Iraqi Journal of Chemical and Petroleum Engineering*, vol. 26, no. 1, pp. 147–153, 2025. https://doi.org/10.31699/ijcpe.2025.1.15

[28] M. Maulani et al., "Optimizing the impact of rheological properties on bentonite pre-hydrated based drilling mud through the utilization of pre-hydration," *IOP Conference Series: Earth and Environmental Science*, vol. 1339, no. 1, 2024. https://doi.org/10.1088/1755-1315/1339/1/012018

[29] H. A. Abbood and S. Al-Anssari, "Enhancement of water-based drilling fluid using novel composite of silica and alumina nanoparticles," *South African Journal of Chemical Engineering*, vol. 57, Jul. 2026. https://doi.org/10.1016/j.sajce.2026.100872

[30] H. A. Abbood and S. Al-Anssari, "Eco-friendly synthesis of silica and alumina from waste materials and their application in improving water-based drilling mud," *Chemical Papers*, May 2026. https://doi.org/10.1007/s11696-026-04922-2

[31] R. Pourrajab, M. Behbahani, and S. N. Moosavi, "Optimizing drilling fluid rheology with hybrid nanoparticles boron nitride and graphene nanosheets: an experimental study," *Scientific Reports*, Apr. 2026. https://doi.org/10.1038/s41598-026-46779-1

[32] Ahmed Hullio, A. H. Tunio, W. Akhtar, M. A. Memon, and N. M. Gabol, "Enhancing the Rheological and Filtration Performance of Water-Based Drilling Fluids Using Silane-Coated Aluminum Oxide NPs," *ACS Omega*, vol. 10, no. 1, pp. 955–963, 2025. https://doi.org/10.1021/acsomega.4c08116

[33] N. Uwaezuoke, U. C. Chukwuebuka, and A. A. Muhammed, "Evaluation of Kaolin Clay Polymeric Nanoparticles for Improved Water-Based Mud Properties," *Oil and Gas: Science and Engineering*, vol. 12, no. 1, pp. 36–45, 2024. https://doi.org/10.11648/ogce.20241201.15

[34] L. Deng et al., "Synthesis and evaluation of selenium-doped nanocomposites in enhancing drilling fluid properties," *Discover Nano*, vol. 21, no. 1, Dec. 2026. https://doi.org/10.1186/s11671-026-04446-4

[35] R. Doukeh et al., "Synthesis, Characterization, and Performance Evaluation of Nanocrystalline Metal Oxides for Shale Inhibition in Water-Based Drilling Fluids," *Sustainable Chemistry*, vol. 7, no. 1, p. 3, Jan. 2026. https://doi.org/10.3390/suschem7010003

[36] A. Gowida, J. P. Shah, and S. Elkatatny, "Foam systems for underbalanced and geothermal drilling: a critical review of stability challenges and research frontiers," *Journal of Petroleum Exploration and Production Technology*, Jan. 2026. https://doi.org/10.1007/s13202-025-02114-4

[37] Q.-B. Wang et al., "Zwitterionic-hydrophobic associating polymer for enhanced rheology and fluid-loss control in high-temperature, high-salinity water-based drilling fluids," *Petroleum Science*, Mar. 2026. https://doi.org/10.1016/j.petsci.2026.03.042

[38] R. Dizayee, J. Ali, and H. Omar, "Performance Impact of the Nano-Colloidal Aphron-Based Drilling Fluids on Rheological and Filtration Properties," *Processes*, vol. 14, no. 4, Feb. 2026. https://doi.org/10.3390/pr14040587

[39] Miao, L. Li, M. Leng, H. Zhang, H. Sun, and B. Huang, "Design and Performance Assessment of a Polymer-Based Filtration-Control System for High-Temperature, High-Density Water-Based Drilling Fluids," *Processes*, vol. 14, no. 9, p. 1326, Apr. 2026. https://doi.org/10.3390/pr14091326

[40] A. Fattah, S. S. Basaloom, M. N. J. AlAwad, F. S. Altawati, and M. A. Almobarky, "Impact of Barite Nanoparticles on Barite Sag in Water-Based Drilling Fluids," *Eng*, vol. 7, no. 3, Mar. 2026. https://doi.org/10.3390/eng7030102

[41] Z. Komekbay et al., "Sublethal Dermal Toxicity of Drilling Fluid and Its Effects on Hematological, Biochemical and Histopathological Parameters in Rats," *Dose-Response*, vol. 24, no. 2, Apr. 2026. https://doi.org/10.1177/15593258261436773

[42] H. Fan et al., "Imbibition and Oil Drainage Mechanisms of Nanoparticle Compound Polymer Fracturing Fluids," *Gels*, vol. 12, no. 2, Feb. 2026. https://doi.org/10.3390/gels12020136

خصائص فائقة لطين الحفر بفعل الاستخدام المستدام للجسيمات النانوية

حسن علي عبود [١، ٢، *]، زين العابدين اراين [٣]، سرمد الانصاري [١، ٢]

١ قسم الهندسة الكيمياوية، كلية الهندسة، جامعة بغداد، العراق
٢ قسم هندسة النفط، كلية الهندسة، جامعة الناجي، العراق
٣ كلية غرب استراليا للمناجم والمعادن والطاقة والهندسة، جامعة كيرتن، ولاية غرب استراليا، استراليا

الخلاصة

تُظهر هذه الدراسة نهجاً مستداماً يعتمد على مبدأ "تحويل النفايات إلى ثروة"، حيث تم تخليق جسيمات السيليكا (SiO_2) والألومينا (Al_2O_3) النانوية بحجم يتراوح بين ٣٠ و٨٠ نانومتر من مواد نفايات محلية— تحديداً طين البنتونايت ونفايات الأسلاك الألومنيوم تقييم أدائها كمضافات صديقة للبيئة في سوائل الحفر ذات الأساس المائي (بحجم ٣٥٠ مل) بتركيزات تراوحت بين ٠ و١ غرام. وعند اختبارها تحت ظروف جوفية قاسية، أدت هذه الجسيمات النانوية المدمجة إلى تحسين الخواص الريولوجية، والقدرة على التزييت، والتحكم في ترشيح السوائل، وتثبيط الانتفاخ بشكل ملحوظ، حيث تضاعف الأداء مع زيادة تركيز الجسيمات النانوية. وبشكل خاص، عند تركيز ١ غرام، ارتفعت نقطة الخضوع (Yield Point) للسائل من خط الأساس ٩ إلى ٤٢ للسيليكا و٣٢ للألومينا، في حين انخفض حجم السائل الراشح تحت ظروف الضغط العالي ودرجة الحرارة العالية (HPHT) من ٢١ مل إلى ١٤,٦ مل للسيليكا و١٦,٤ مل للألومينا نتيجة تشكّل كعكة ترشيح منخفضة النفاذية. علاوة على ذلك، ساهم تركيز ٠,٧٥ غرام في خفض معامل الاحتكاك من ٠,٤٥ إلى ٠,٣٥ للسيليكا و٠,٣٧ للألومينا، مع الحد بفعالية من انتفاخ الطين (حيث أظهرت نانو السيليكا تثبيطاً فائقاً عند التركيزات الأقل)، مما يثبت في النهاية أن هذه الجسيمات النانوية المستخلصة من النفايات توفر بديلاً عالي الكفاءة، واقتصادياً، وصديقاً للبيئة للمضافات التجارية المستخدمة في طين الحفر.

الكلمات الدالة: التخليق المستدام، السيليكا، الألومينا، الجسيمات النانوية، طين الحفر.